Mapping the Development of Cerebellar Purkinje Cells in Zebrafish

Kyla R. Hamling, Zachary J.C. Tobias, Tamily A. Weissman

Department of Biology, Lewis & Clark College, Portland, Oregon 97219

Received 17 October 2014; revised 6 January 2015; accepted 7 January 2015

ABSTRACT: The cells that comprise the cerebellum perform a complex integration of neural inputs to influence motor control and coordination. The functioning of this circuit depends upon Purkinje cells and other cerebellar neurons forming in the precise place and time during development. Zebrafish provide a useful platform for modeling disease and studying gene function, thus a quantitative metric of normal zebrafish cerebellar development is key for understanding how gene mutations affect the cerebellum. To begin to quantitatively measure cerebellar development in zebrafish, we have characterized the spatial and temporal patterning of Purkinje cells during the first 2 weeks of development. Differentiated Purkinje cells first emerged by 2.8 days post fertilization and were spatially patterned into separate dorsomedial and ventrolateral clusters that merged at around 4 days. Quantification of the Purkinje cell layer revealed that there was a logarithmic increase in both Purkinje cell number as well as overall volume during the first 2 weeks, while the entire region curved forward in an anterior, then ventral direction. Purkinje cell dendrites were positioned next to parallel fibers as early as 3.3 days, and Purkinje cell diameter decreased significantly from 3.3 to 14 days, possibly due to cytoplasmic reappropriation into maturing dendritic arbors. A nearest neighbor analysis showed that Purkinje cells moved slightly apart from each other from 3 to 14 days, perhaps spreading as the organized monolayer forms. This study establishes a quantitative spatiotemporal map of Purkinje cell development in zebrafish that provides an important metric for studies of cerebellar development and disease. © 2015 Wiley Periodicals, Inc. Develop Neurobiol 75: 1174–1188, 2015

Keywords: **cerebellum; development; Purkinje cell; parvalbumin7; zebrafish**

INTRODUCTION

Motor behaviors require precise control and coordination by the nervous system. Even for the simplest motor tasks in vertebrates, the brain must integrate sensory and motor information and coordinate multiple groups of muscles throughout the body to achieve an accurate, unified movement. This crucial integration is performed by the cerebellum. The cerebellum is found in every vertebrate animal and its basic cellular organization is highly conserved across species (Bell, 2002), implying the importance of the cerebellum's role in behavior throughout vertebrate evolution. Beyond its importance for understanding motor control and behavior, the cerebellum's relative simplicity allows insight into how a relatively simple circuit is able to regulate complex behavior with only a discrete number of cell types. As such, the cerebellum is an ideal target for studying the general concepts that underlie the development of complex circuits in the brain (van Welie et al., 2011).

Of the main cell types in the cerebellum, the Purkinje cell ultimately determines cerebellar output, and is therefore one of the most developmentally characterized cell types thus far. In both mammalian and teleost species, Purkinje cells are produced in the ventricular zone of the fourth ventricle by progenitor cells expressing the pancreatic transcription factor 1a proneural gene (ptf1a) (Hoshino et al., 2005; Hoshino, 2006; Kani et al., 2010). Immature Purkinje cells

Correspondence to: T. A. Weissman (weissman@lclark.edu).
Contract grant sponsor: National Science Foundation.
Contract grant sponsor: M. J. Murdock Charitable Trust.

Published online 18 February 2015 in Wiley Online Library (wileyonlinelibrary.com).
DOI 10.1002/dneu.22275

migrate dorsally away from the ventricular zone toward the Purkinje cell layer where they differentiate into mature neurons (Miale and Sidman, 1961; Yuasa et al., 1991; Kani et al., 2010). The Purkinje cell plays an important role in spatially regulating the development of other cerebellar cell types (Wechsley-Reya and Scott, 1999; Lewis et al., 2004; Fleming et al., 2013; White et al., 2014), helping to ensure proper formation of the functional circuit. For example, Purkinje cells are necessary for maintaining normal granule cell number (Goldowitz and Hamre, 1998). Understanding the principles that guide proper development of each of these cerebellar cell types is important for understanding not only how one cell type develops spatiotemporally, but also how the circuit develops as a whole.

Although cerebellar development has been studied extensively in mammals, less is known about its development in nonmammalian model organisms such as zebrafish. The fundamental cerebellar circuitry is conserved between mammals and teleosts (Bae et al., 2009; Kani et al., 2010), making zebrafish a useful model for studying cerebellar cell types and their interactions during development, adulthood, and disease. Due to their basic similarities with other vertebrates, along with their transparency during development and genetic tractability, zebrafish have emerged as a powerful model system in which human mutations can be recapitulated and studied *in vivo* (reviewed in Lieschke and Currie, 2007). Interestingly, despite their similarities to mammals, recent studies have demonstrated certain key evolutionary differences in cerebellar development that exist in teleosts, such as the lack of an external granule layer in the teleost cerebellum (Chaplin et al., 2010). In mammals, the proliferation of granule cells through sonic hedgehog signaling in the external granule cell layer leads to the characteristically extensive foliation of the cerebellum (Corrales et al., 2004, 2006); species with increased degree of cerebellar foliation have been shown to exhibit more complex behaviors in studies across both avian and batoid species (Lisney et al., 2008; Iwaniuk et al., 2009; Hall et al., 2013). Studying the divergence in developmental plans between the teleostean and mammalian cerebellum therefore may elucidate both molecular and behavioral pathways in vertebrate evolution.

Initial characterization of the adult and larval zebrafish cerebellum has begun (Miyamura and Nakayasu, 2001; Bae et al., 2009; Kani et al., 2010; Volkmann et al. 2008, 2010; Hibi and Shimizu, 2012; Kaslin et al., 2013). Given the behavioral and evolutionary importance of this circuit, and its vulnerability to developmental disorders (Gosalakkal, 2001; Picard et al., 2008; Fatemi et al., 2012), a detailed map of normal cerebellar development would be a powerful additional tool. In this study, we provide a detailed spatiotemporal map of the cerebellar Purkinje cell along with its presynaptic input, the granule cell parallel fiber, during the first 2 weeks of zebrafish development that can be used as a standard for future studies.

METHODS

Zebrafish Maintenance

Wild type zebrafish (*Danio rerio*; AB/TL; Westerfield, 2000; Zebrafish International Resource Center, Eugene, OR) were housed in a circulating tank system (Aquaneering, San Diego, CA) held at 28°C and dosed to maintain pH and salinity. Embryos were raised in E3 embryonic medium (Nüsslein-Volhard and Dahm, 2002) in an incubator or fish room held at 28°C. To prevent pigmentation, zebrafish larvae were exposed to 0.2 m*M* phenylthiourea beginning at 24 h post fertilization (hpf). To remove pigmentation, some fish were treated with 3% hydrogen peroxide and 1% KOH for 30 min postmortem. Female and male fish were pooled in the analysis. Zebrafish developmental stages were determined as described previously (Kimmel et al., 1995). Zebrafish are classified as embryos before 3 days post fertilization (dpf), and larvae between the ages of 3 and 29 dpf. All experimental methods were approved by the Institutional Animal Care and Use Committee of Lewis & Clark College.

Developmental Time Points

Embryos were fixed for immunohistochemistry at each day through 7 dpf, and then again at 14 dpf to cover a wide developmental time span extending from before Purkinje cells were expected to differentiate until substantially after the nascent circuit had initially formed. Additional time points were fixed at 2.3, 2.8, 2.9, and 3.3 dpf (54, 67, 70, and 80 h post fertilization respectively) to create a finer temporal map of development. Here, larval ages will be referred to in dpf, with precise dpf time points (3 dpf, 4 dpf, etc.) referring to the exact hours post fertilization (hpf) correlate (72 hpf, 96 hpf, etc.).

Immunohistochemistry

For whole-mount immunostaining, zebrafish larvae were fixed in 4% paraformaldehyde at 4°C overnight. Fixed larvae were then washed with PBST (phosphate-buffered saline, 0.1% TritonX-100) three times and then incubated in 100% acetone at −20°C for 15 min. Following permeabilization, samples were rinsed with PBST for 5 min, and PBSDT (phosphate-buffered saline, 0.1% TritonX-100, 0.1% DMSO) for 5 min. Samples were then incubated in blocking solution (PBS, phosphate-buffered saline, 5% normal goat serum, 1% TritonX-100, 1% BSA, 1% DMSO) at room temperature (RT) for 1 h before being transferred to the primary antibody (Table 1) diluted in antibody buffer

Table 1 Primary Antibodies Used

Name	Immunogen	Manufacturer	Dilution
Anti-Pvalb7	Amino acids 1–109 of *Danio rerio* parvalbumin7 (NP_991137)	Dr. Masahiko Hibi, mouse monoclonal	1:1500
Anti-VGlut1	Synthetic peptide, CVGTNSYLYGGEGERELT	Dr. Masahiko Hibi, rabbit polyclonal	1:1000

(PBS, 1% normal goat serum, 0.2% TritonX-100, 0.2% BSA, 0.2% DMSO, 0.05% sodium azide) and incubated on a shaker at RT overnight. Following a 1-h wash with PBST, samples were incubated with the secondary antibody solution (1:1000 dilution in antibody buffer, AlexaFluor488, AlexaFluor555, or AlexaFluor633 goat antimouse and/or goat antirabbit; Life Technologies) on a shaker for 2 h at RT. Whole mounts were rinsed with PBS for 1 h, then transferred to PBS for long-term storage at 4°C.

Antibody Characterization

All antibodies were found to label cell types in a manner consistent with previous antibody characterizations (Table 1). Anti-parvalbumin7 (Pvalb7) has been previously characterized in detail (Bae et al., 2009) and shown to label the soma, axon, and dendrites of cerebellar Purkinje cells and crest cells. Anti-Pvalb7 labeling is consistent with expression of Pvalb7 mRNA transcripts in adult zebrafish and with other Purkinje cell antibody markers (Bae et al., 2009). Anti-Pvalb7 has previously been used in several studies to identify Purkinje cells in zebrafish (Tanabe et al., 2010; Yanicostas et al., 2012; Kaslin et al., 2013). Anti-vesicular glutamate transporter type 1 (VGlut1) has been previously characterized and shown to label the axon terminals of granule cells in the corpus cerebellum, eminentia granularis (EG), and caudal lobe (LCa) of the zebrafish cerebellum (Bae et al., 2009). The anti-VGlut1 antibody recognizes one band of 64 kDA on an immunoblot of zebrafish brain lysates (Bae et al., 2009).

Microscopy

For whole-mount procedures, fish were embedded in 1% low-melt agarose (Amresco© Agarose super fine resolution diluted in reverse osmosis purified water) for the duration of imaging. Images were taken on a Zeiss LSM710 laser-scanning confocal microscope (20× water, 1.0 NA objective). A 488 nm laser line was used for imaging AlexaFluor488, 561 nm laser line used for imaging AlexaFluor555, and 633 nm laser line used for imaging AlexFluor633. Transmitted light images of immunostained zebrafish were also taken on a Zeiss Discovery V8 fluorescence dissection microscope for anatomical measurements.

Image Processing, Quantification, and Statistical Analysis

Purkinje cell layer anterior–posterior length (AP length) was determined as the distance from most rostral to most caudal cell in the medial portion of the cerebellum. Purkinje cell layer lateral width was determined as distance from most lateral edge of the cerebellum to the opposite lateral edge. Purkinje cell layer height was measured as distance from most dorsal cell to most ventral cell within the cerebellum. Purkinje cell layer lateral width and AP length measurements were calculated using the measure tool in ImageJ on confocal projections. Purkinje cell layer height was determined by the number of 1.00 μm optical sections between the most ventral Purkinje cell body and the most dorsal Pvalb7 signal. Volume calculations were made using the Volumest ImageJ plug-in (Merzin, 2008). Number of Purkinje cell bodies within the Purkinje cell layer was determined by scrolling through an optical stack and placing regions of interest (ROIs) in the center of an in-focus cell body in ImageJ. Nearest neighbor distances were then calculated from the ROI overlay using the Nearest Neighbor Distance ImageJ plugin (Yuxiong Mao). Cell body diameter and roundness were measured using sagittal confocal images acquired with a 20× water objective (1.0 NA) at 5× zoom. Cell body diameter was determined by measuring the longest axis of the cell body in ImageJ. Cell body roundness was measured using the ImageJ "roundness" shape descriptor of a freehand selection around the cell body perimeter. The longest axis of the cell was compared to its shortest axis, and "roundness" was calculated on a scale from 1 to 0, where "1" reflects the two axes being equal (perfectly round/proportional), and values closer to "0" reflect a more oblong cell. Throughout the manuscript, statistical significance was determined using a linear or logarithmic regression. Statistical error is reported as standard deviation. For image clarity during analysis, image levels were adjusted in ImageJ; images used to quantify Purkinje cell layer volume and cell number were all adjusted to the same gamma level (0.5) before quantification, which is appropriate within the context of these experiments as signal brightness was not being quantified and compared.

RESULTS

Spatial and Temporal Patterning of Purkinje Cells

To determine when and where Purkinje cells first differentiate during cerebellar development, we examined the expression of the Purkinje cell-specific, intracellular Ca^{2+} buffer protein, parvalbumin-7 (Pvalb7), in embryonic and larval zebrafish at various time points between 1 and 14 dpf using whole-mount

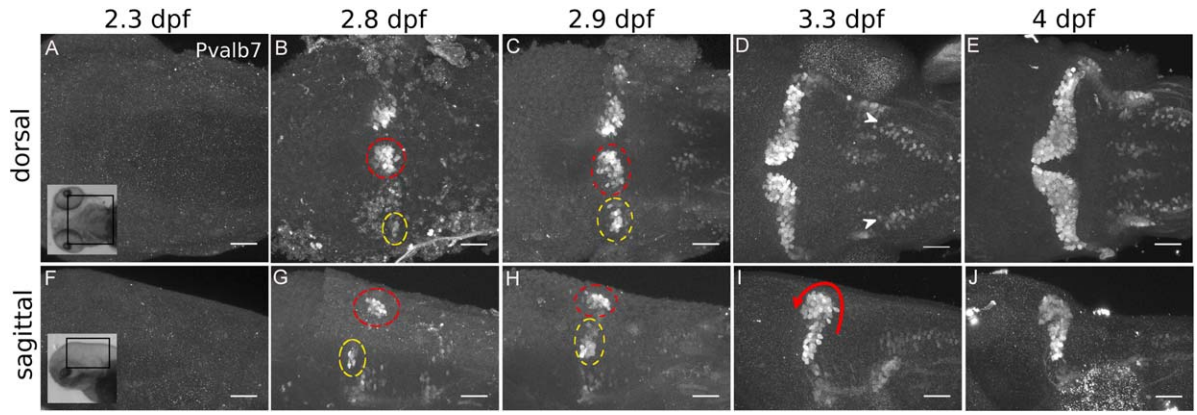

Figure 1 Parvalbumin7 expression reveals Purkinje cell development between 2.3 and 4 dpf. Maximum intensity projections of confocal image stacks (roughly 200 μm in depth) of Pvalb7 expression from dorsal (A–E) and sagittal (F–J) views between 2 and 4 dpf. Insets show approximate dorsal and sagittal brain region imaged (A, F). Pvalb7 expression was seen by 2.8 dpf (67 hpf) in a dorsomedial cluster (red dashed circle) and ventrolateral cluster (yellow dashed circle). These clusters became less distinct by 2.9 and 3.3 dpf (70 and 80 hpf; C, D, H, I) and appeared to merge by 4 dpf (E, J), while the Purkinje cells begin to curve forward (I, curving arrow). A population of dorsolateral hindbrain Pvalb7-expressing neurons was present by 3.3 dpf (D, white arrowheads). Scale bar 50 μm. Images taken using 20× (1.0 NA) water objective. [Color figure can be viewed in the online issue, which is available at wileyonlinelibrary.com.]

immunohistochemistry. Pvalb7 protein signal was absent at 1, 2, and 2.3 dpf [54 hpf; Fig. 1(A,F)], and was first seen at 2.8 dpf [67 hpf; Fig. 1(B,G)]. Within this region of the cerebellum, Pvalb7 expresses only in differentiated Purkinje cells (Bae et al., 2009; Kani et al., 2010) indicating that immature Purkinje cells in the cerebellum began differentiating between 2.3 and 2.8 dpf. This is slightly earlier than the previously reported date, which placed Purkinje cell differentiation at 3 dpf (Bae et al., 2009).

By 2.8 dpf (67 hpf), Purkinje cell bodies were found in a distinct, bilaterally symmetrical pattern directly posterior to the midbrain-hindbrain boundary and anterior to the fourth ventricle [Fig. 1(B,G)]. At this early developmental time point, Purkinje cells in each brain hemisphere appeared to be spatially patterned into two distinct clusters: a larger, dorsomedial cluster and a smaller, ventrolateral cluster [Fig. 1(B,G); red and yellow dashed circles, respectively]. By 2.9 dpf [70 hpf; Fig. 1(C,H)], these clusters became less distinct as differentiated cells began to appear between these clusters. The clusters became nearly unified by 3.3 dpf (80 hpf), when the Purkinje cell bodies now formed a continuous layer that spanned the mediolateral width of the brain [Fig. 1(D,I)]. By 4 dpf, the Purkinje cell clusters were completely merged, and the Purkinje cell layer had adopted its characteristic wing-shaped morphology [Fig. 1(E,J)].

Our investigation of the expression of Pvalb7 in differentiated Purkinje cells between 1 and 4 dpf indicated that the wing-shaped Purkinje cell layer morphology was present as early as 4 dpf. We next asked how gross morphology of the Purkinje cell layer changes once the differentiated Purkinje cells are in place. In order to answer this question, we followed the expression of Pvalb7 in the Purkinje cell layer from 4 through 14 dpf (Fig. 2). While the bilateral wing-shaped morphology of the Purkinje cell layer remained present between 4 and 14 dpf [Fig. 2(A–E)], there were more subtle changes in the spatial patterning of the Purkinje cells during this time period. When examining the differentiated Purkinje cells from a sagittal view [Fig. 2(F–I)], it became apparent that the entire Purkinje cell layer was progressively curving in the anterior and subsequently ventral direction. This curving began as early as 3.3 dpf [Fig. 1(I), curving arrow] and progressed to form a broad, inverted-U shape curve by 7 dpf [Fig. 2(I)] that was morphologically similar to the curve of the adult zebrafish cerebellum. This curving also coincided with an outgrowth of presumptive cerebellovestibular efferent tracts that began as early as 5 dpf and was well established by 7 dpf [Fig. 2(I); yellow arrowheads]. Additionally, Pvalb7 expression was found in a population of dorsolateral hindbrain cells lining the ventricle on either side of the brain, beginning at 3.3 [Fig. 1(D)] and continuing through 14 dpf [Fig. 2(A–E); white arrowheads in 1(D) and 2(A)], possibly representing Pvalb7-expressing crest cells in the medial octavolateral nucleus (Bae et al., 2009).

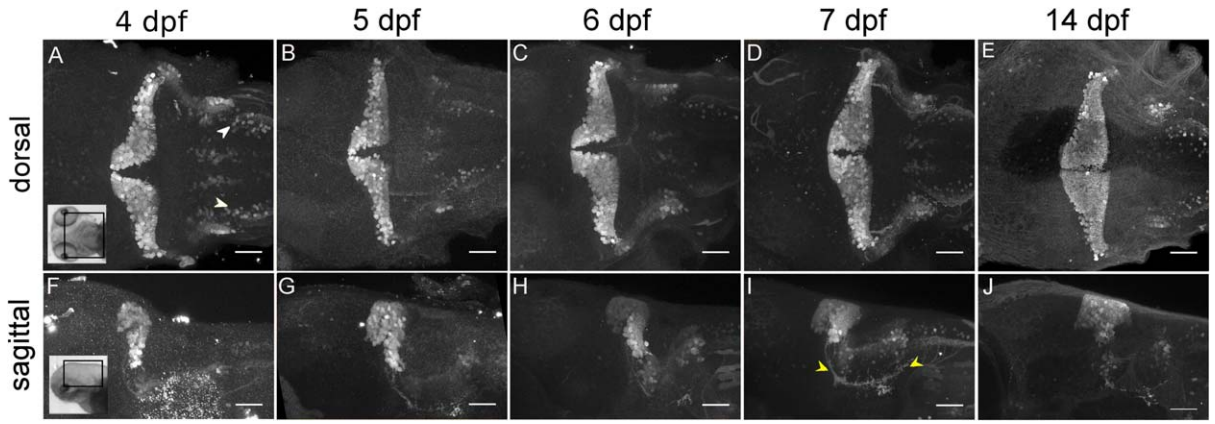

Figure 2 Parvalbumin7 expression reveals morphological changes in the Purkinje cell layer between 4 and 14 dpf. Maximum intensity projections of Pvalb7 expression from dorsal (A–E) and sagittal (F–I) views in 4–14 dpf larvae. Insets represent approximate dorsal and sagittal brain region imaged (A, F). The wing-shaped morphology of the Purkinje cell layer is present at all developmental time points (A–E), though it begins to wrap more anteriorly (see G–I) and Purkinje cells begin to project cerebellovestibular axons (yellow arrowheads) by 7 dpf (I). Dorsolateral hindbrain neurons are present by 4 dpf (A, white arrowheads). Scale bar 50 μm. Images taken using 20× (1.0 NA) water objective. [Color figure can be viewed in the online issue, which is available at wileyonlinelibrary.com.]

Quantification of Purkinje Cell Layer Developmental Changes

To quantify the qualitative observations of Purkinje cell layer shape and size between differentiation and 14 dpf, we acquired confocal images of Pvalb7 expression and measured the following dimensions: Purkinje cell layer anterior–posterior length [distance from most rostral to most caudal cell in the medial portion of the Purkinje cell layer; Fig. 3(A)]; lateral width [distance from most lateral edge to the opposite lateral edge of Purkinje cell layer; Fig. 3(A)]; Purkinje cell layer height [distance from most dorsal cell to most ventral cell; Fig. 3(B)]; and total volume of the Purkinje cell layer.

Between 2.8 and 14 dpf, a linear regression analysis showed that larval age predicted AP length of the Purkinje cell layer [Fig. 3(C)]. AP length increased significantly in a linear manner by 3.6 μm per day ($p = 0.000016$), increasing 46.1% from 57.0 (±9.9) μm at 2.8 dpf ($n = 3$) to 83.3 (±5.7) μm at 14 dpf ($n = 3$). This increase was consistent with the Purkinje cell layer curving anteriorly during the same time period (Figs. 1 and 2).

Purkinje cell layer lateral width did not significantly change with increasing larval age between 2.8 and 14 dpf [$p = 0.09$; Fig. 3(D)]. During early development, the Purkinje cells spanned nearly the entire brain; the lateral width of the head therefore represented the upper limit of the Purkinje cell layer lateral width. The lateral width of the larval head also did not significantly change during this time period ($p = 0.71$; data not shown), consistent with a lack of lateral Purkinje cell layer expansion with age. Purkinje cell layer height also did not significantly change with increasing age [$p = 0.18$; Fig. 3(E)].

Finally, our analysis of the volume of the Purkinje cell layer between 2.8 and 14 dpf revealed that overall volume increased logarithmically with increasing larval age [Fig. 3(F); $p = 1.7 \times 10^{-9}$]. The largest increase in Purkinje cell layer volume occurred between 3.3 and 4 dpf, when the average volume increased 75.9% from 250,250 (±53,839) μm^3 ($n = 2$) to 440,280 (±48,708) μm^3 ($n = 5$). Purkinje cell layer volume increased more slowly after 4 dpf, by an average of only 2.2% each day.

Characterizing Individual Purkinje Cells in the Purkinje Cell Layer

The nonlinear trend of Purkinje cell layer volume increase that we observed was unexpected, namely an initial large increase followed by a plateauing increase (fitted here with a logarithmic function). Several hypotheses were generated to possibly explain this phase: (1) Purkinje cells differentiate at a logarithmic rate, meaning fewer Pvalb7-expressing cells appear in the Purkinje cell layer at later time points; (2) over time, Purkinje cells differentiate at a constant rate, but their cell bodies become smaller, taking up less volume at later time points; (3) Purkinje cells differentiate a constant rate, but the cells

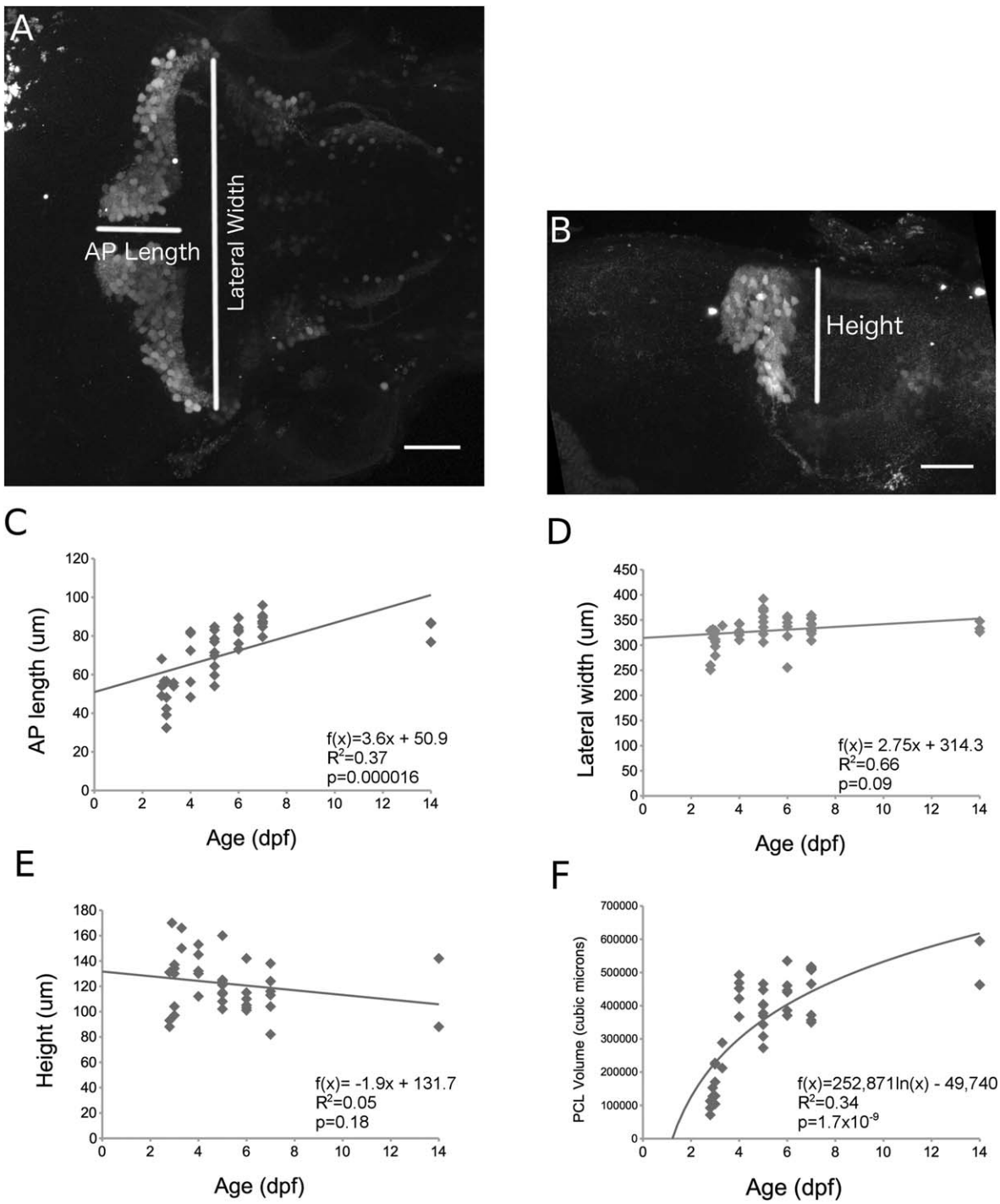

Figure 3 Average Purkinje cell layer anterior–posterior length and volume change during early development. Sample image shows anterior–posterior length (AP length), lateral width (A) and height (B) measurements in a 5 dpf larva. (C) Scatter plot of AP length (μm) between 2.8 and 14 dpf. AP length increased linearly with increasing age ($p = 0.000016$). (D) Lateral width (μm) did not significantly change between 2.8 and 14 dpf ($p = 0.09$). (E) Purkinje cell layer height did not significantly change with age ($p = 0.18$). (F) Purkinje cell layer (PCL) volume (μm^3) increased logarithmically between 2.8 and 14 dpf ($p = 1.7 \times 10^{-9}$). Curve estimates represent linear (C, D, E) or logarithmic regression (F). Scale bars 50 μm. Images taken using 20× (1.0 NA) water objective. Sample sizes for each time point (number of animals) are as follows: 2.8 dpf = 3; 2.9 dpf = 2; 3 dpf = 5; 3.3 dpf = 2; 4 dpf = 5; 5 dpf = 9; 6 dpf = 6; 7 dpf = 8; 14 dpf = 3. In 3E, 5 dpf = 8. In 3D, 7 dpf = 9. In 3E, 14 dpf = 2. [Color figure can be viewed in the online issue, which is available at wileyonlinelibrary.com.]

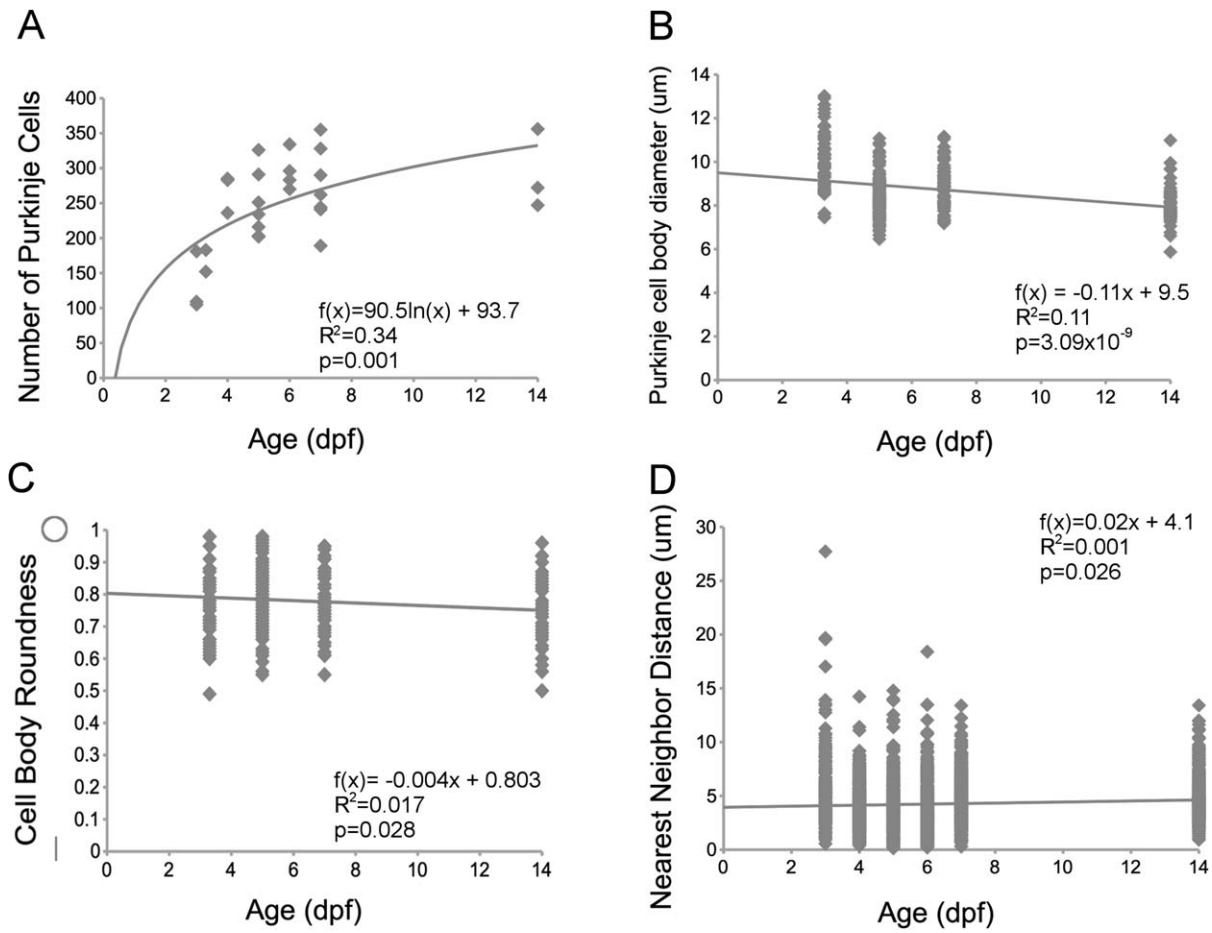

Figure 4 Quantification of Purkinje cell number, diameter, cell roundness and nearest neighbor reflect changes in the Purkinje cell layer. (A) Scatter plot of number of cell bodies in the Purkinje cell layer between 3 and 14 dpf. Number of cell bodies increased logarithmically with increasing age ($p = 0.001$). (B) Purkinje cell body diameter (μm) decreased significantly between 3.3 and 14 dpf ($p = 3.09 \times 10^{-9}$). (C) Purkinje cell body roundness decreased between 3.3 and 14 dpf ($p = 0.028$). (D) Distance to nearest neighboring cell body increased significantly between 3 and 14 dpf ($p = 0.026$). Curve estimates represent linear (B, C, D) or logarithmic (A) regression. Sample sizes for each time point (number of animals) are as follows: In 4A, 2.8 dpf = 2; 2.9 dpf = 2; 3 dpf = 3; 3.3 dpf = 2; 4 dpf = 3; 5 dpf = 7; 6 dpf = 4; 7 dpf = 7; 14 dpf = 3. In 4B, 3.3 dpf = 63 cells, from 3 fish; 5 dpf = 114,3; 7 dpf = 73,3; 14 dpf = 52,2. In 4C, 3.3 dpf = 59,3; 5 dpf = 112,3; 7 dpf = 71,3; 14 dpf = 42,2. In 4D, 3 dpf = 389,3; 4 dpf = 548,2; 5 dpf = 450,2; 6 dpf = 597,2; 7 dpf = 706,2; 14 dpf = 875,3.

pack more closely together within the Purkinje cell layer over time; or (4) some combination of these possibilities. To determine which of these possible hypotheses was underlying the logarithmic nature of Purkinje cell layer growth, we carefully quantified spatiotemporal patterns of the individual Purkinje cells that make up the Purkinje cell layer between days 3 and 14.

To first determine whether new Purkinje cells were differentiating during the plateau phase, we quantified the average number of Pvalb7-expressing cell bodies in the Purkinje cell layer at each time point [Fig. 4(A)]. Like volume, the number of cell bodies increased logarithmically with age ($p = 0.001$). The greatest increase in Purkinje cells occurred between 3 and 4 dpf, increasing 103.6% from an average of 131.6 (±42.8) cell bodies in the Purkinje cell layer at 3 dpf ($n = 3$) to 268 (±27.7) cell bodies at 4 dpf ($n = 3$).

We next quantified the average diameter of individual cell bodies within the Purkinje cell layer at 3.3, 5, 7, and 14 dpf. A linear regression analysis showed that Purkinje cell body diameter decreased significantly with age [$p = 3.09 \times 10^{-9}$; Fig. 4(B)]. Cell body diameter decreased 18% over this time period, from 9.9 (±1.3) μm at 3.3 dpf ($n = 59$ cells;

three animals) to 8.1 (±0.8) μm at 14 dpf ($n = 52$ cells; two animals). We also quantified cell roundness to determine whether the change in cell body diameter was due to a change in cell shape. A linear regression analysis showed a small but significant decrease in cell roundness (becoming more oval) from 3.3 to 14 dpf [$p = 0.028$; Fig. 4(C)]. This shape change is unlikely to explain a decrease in cell body diameter, however, as cell diameter was measured along the cell body's longest axis for this analysis.

To address whether the cell bodies were packing more closely together during development or spreading apart, we quantified the distance to the nearest neighboring Purkinje cell in the Purkinje cell layer between days 3 ($n = 281$ cells; two animals) and 14 ($n = 875$ cells; three animals). A linear regression analysis revealed that nearest neighbor distance increased significantly with age ($p = 0.026$), by 0.022 μm per day [Fig. 4(D)], showing that as the cerebellum developed, Purkinje cells spread slightly further apart from each other. Taken together, as the cerebellum developed from 3 to 14 days, differentiated Purkinje cells increased in number in the Purkinje cell layer at a logarithmic rate, decreased in cell diameter, became slightly less round, and spread apart from each other, thus contributing to the overall increase in volume of the region that we measured.

To examine the morphology of individual Purkinje cells in greater detail, confocal images of Pvalb7-immunostained larva were taken at high magnification at 3.3, 5, and 7 dpf (Fig. 5). Images were taken from a sagittal view, to visualize the cell body and dendrites of a single Purkinje cell. Images were consistently acquired at the most lateral portion of the Purkinje cell layer to minimize variability in dendritic development that may occur spatially within the cerebellum, as previous studies in zebrafish have reported that Purkinje cell dendrites in the medial portion of the cerebellum are not planar and are irregularly packed, whereas dendrites in the lateral portion are planar and resemble mammalian dendritic arbors (Miyamura and Nakayasu, 2001).

Early in development at 3.3 dpf, Pvalb7 expression was visible in cell bodies but not in primary dendrites [Fig. 5(A)]. There was a region of nonsomatic, diffuse Pvalb7 signal dorsal to these cell bodies, potentially representing developing neurites [Fig. 5(A_1); white dashed region]. By 5 dpf, we found that Pvalb7 was expressed in immature dendritic projections [Fig. 5(B)], consistent with previous findings (Tanabe et al., 2010). Immature dendrites expanded by 7 dpf into a more developed arbor, including both a single primary dendrite and branched secondary dendrites [Fig. 5(C)].

Spatial and Temporal Patterning of Parallel Fibers

Having comprehensively quantified the spatial and temporal patterns of Purkinje cell morphology and Pvalb7 expression during the first 2 weeks of larval development, we began to characterize the granule cell parallel fibers, which synapse onto Purkinje cells in the molecular layer. To determine where and when the parallel fibers develop in relation to Purkinje cells, we performed immunostaining against both Pvalb7, to visualize differentiated Purkinje cells, and vesicular glutamate transporter type 1 (VGlut1), which localizes to granule cell axons (presynaptic parallel fibers).

Like Pvalb7, VGlut1 expression was not seen before 2.8 dpf. Previous literature reports that immature granule cells leave the upper rhombic lip and begin migrating into place at 2 dpf (Köster and Fraser, 2006; Volkmann et al., 2008), suggesting that the granule cell axons take somewhere up to 0.8 days to form and begin expressing VGlut1. At 2.9 dpf, VGlut1 expression was visible mainly lining the ventricle, at the posterior portion of the developing cerebellum [Fig. 6(A,B)]. By this time, the population of parallel fibers had begun to send projections posteriorly from the cerebellum [Fig. 6(A_1,B_1); white arrowheads]. This early-emerging population of parallel fibers may originate from granule cells in the prospective EG or LCa, as these regions project axons posteriorly to the cerebellum-like structure, the crista cerebellaris (CC) (Volkmann et al., 2008; Hibi and Shimizu, 2012). A small amount of the VGlut1 expression at 2.9 dpf, however, could be found extending anteriorly at the most medial portion of the cerebellum. This population of parallel fibers may correspond to projections from granule cells within the developing corpus cerebelli (CCe), as the CCe sends parallel fibers only to Purkinje cells within the cerebellum itself (Bae et al., 2009).

When compared to the expression of Pvalb7 at this time point, VGlut1 expression appeared just posterior to the differentiated Purkinje cells [Fig. 6(A3)] and extended further dorsally [Fig. 6(B3)] than Pvalb7 expression. There was little spatial overlap between VGlut1 expression in parallel fibers and Purkinje cells except at the most lateral regions of the cerebellum. Twelve hours later, by 3.3 dpf, VGlut1 signal had increased drastically. The parallel fibers in the presumptive CCe had expanded their territory anteriorly toward the midbrain-hindbrain boundary, but did not yet form a continuous layer in this region [Fig. 6(C)]. Additionally, there was a substantial outgrowth of granule cell axons projecting posteriorly

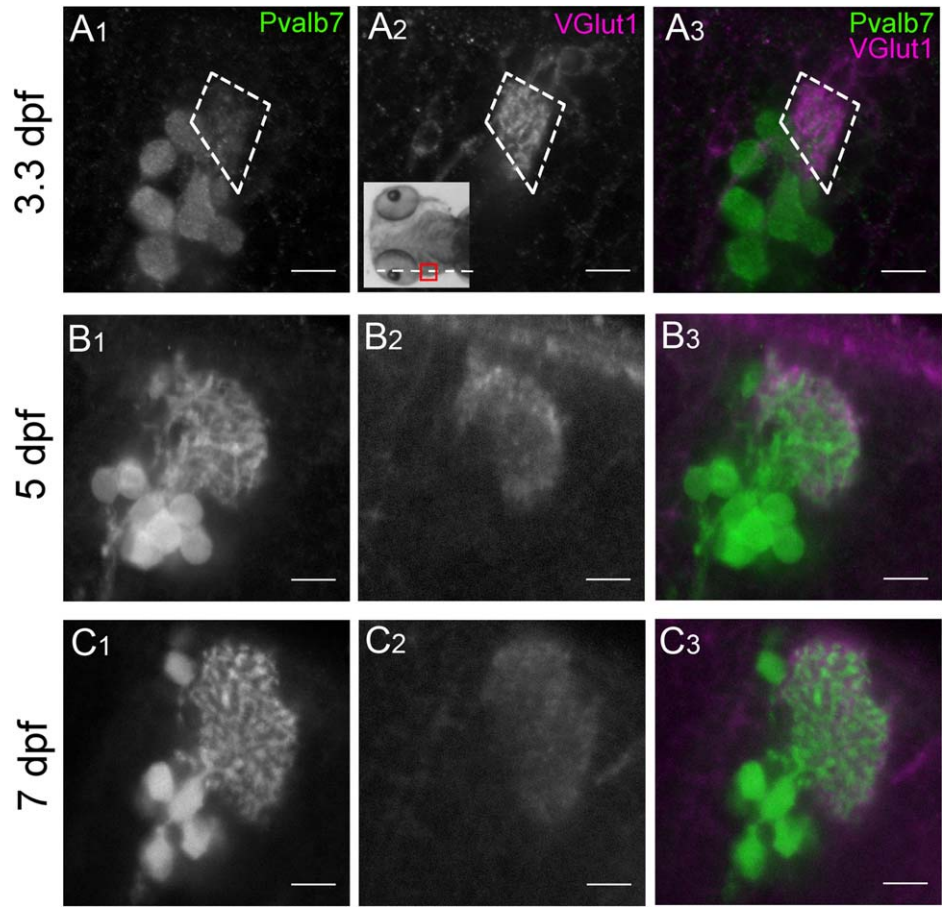

Figure 5 Purkinje cell dendritic arbor develops over time. (A) Pvalb7 and VGlut1 expression in Purkinje cells at 3.3 dpf (80 hpf). Pvalb7 (A1), Vglut1 (A2) expression, and merge of channels (A3) shows that Pvalb7 is expressed in cell bodies but no visible primary dendrites, and that VGlut1 is found directly dorsal to Purkinje cell bodies and overlapping with some possible Pvalb7 expression in neuropil (white dashed region). (B1–3) By 5dpf, the immature dendrites are also overlapping with the expanded VGlut1 expression in parallel fibers. (C1–3) By 7dpf, the Purkinje cell dendrite has grown dorsally and the VGlut1 layer has expanded accordingly to remain overlapping. Inset in A2 shows rough location of sagittal plane of section (indicated by dashed line). Scale bar 10 μm. Images taken using 20× (1.0 NA) water objective, at 5× zoom. [Color figure can be viewed in the online issue, which is available at wileyonlinelibrary.com.]

out of the cerebellum [Fig. 6(C1,D1); white arrowheads]. When examining the expression of both VGlut1 and Pvalb7 together [Fig. 6(C3,D3)], there was a moderate degree of signal overlap—parallel fibers and Purkinje cells were found in the same wing-shaped layer, with parallel fibers found more dorsal to Purkinje cells.

By 5 days, VGlut1 expression was found evenly throughout the anterior–posterior axis of the cerebellum [Fig. 6(E,F)], indicating that parallel fibers have formed a continuous molecular layer. Importantly, by 5 dpf, VGlut1 expression in the molecular layer began to curve anteriorly [Fig. 6(F)], following the morphological changes on the Purkinje cell layer at this time point. These data are consistent with the development of the laminar structure of the cerebellum (Bae et al., 2009): by 5dpf, parallel fibers appeared to be spatially coordinated with Purkinje cells and located just dorsal to the cells [Fig. 6(E3,F3)], and were even forming primitive layers by 3.3 dpf. This spatial coordination of the Purkinje cell layer and the molecular layer remained present at all time points through 14 dpf (data not shown).

Examining the expression of Pvalb7 and VGlut1 together suggested that the zebrafish cerebellum formed primitive layers by 3.3 dpf and that Purkinje cells and parallel fibers were highly spatially coordinated by 5 dpf, with significant signal overlap. Is this

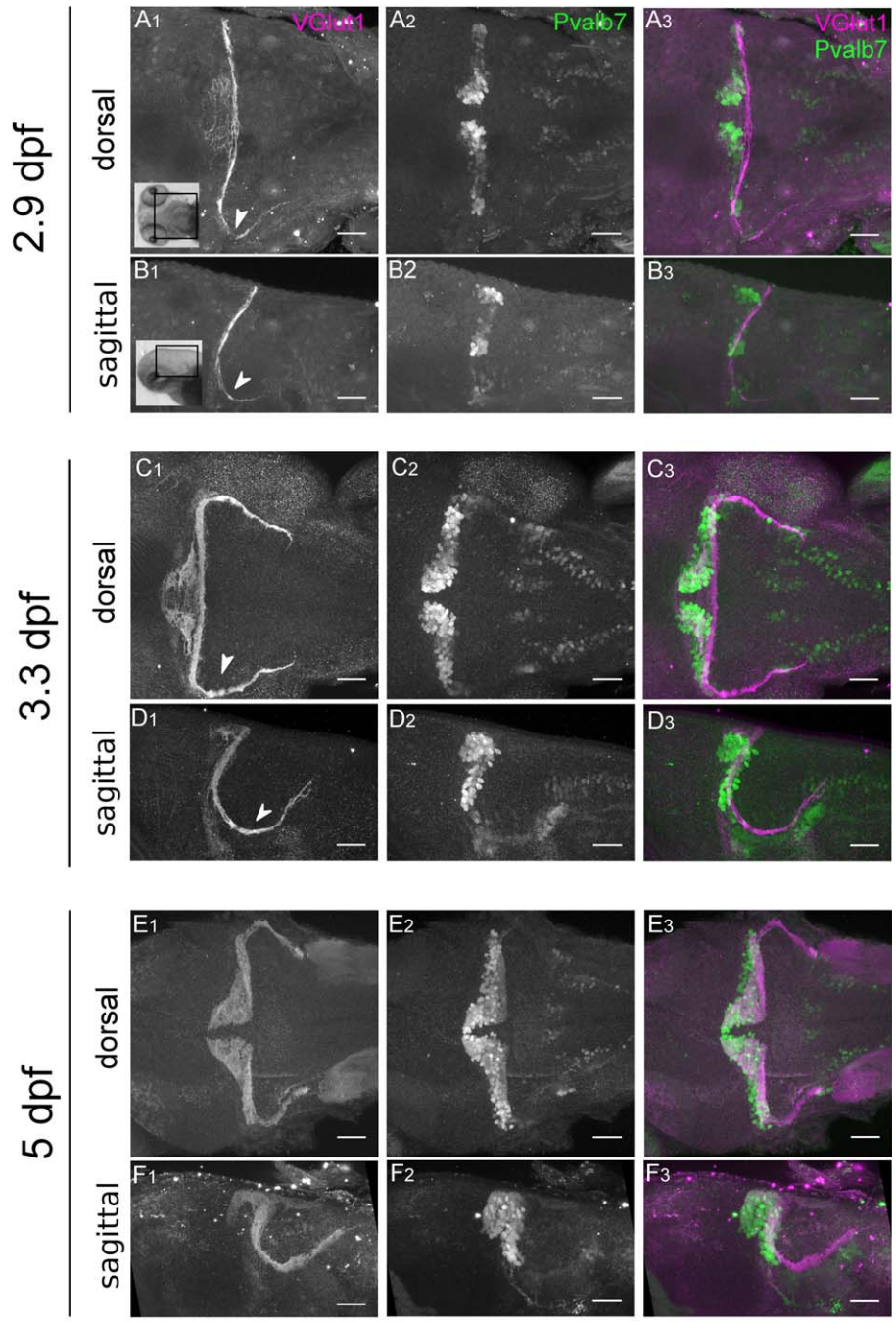

Figure 6 Vglut1 expression in parallel fibers moves anteriorly early in development and coincides with Purkinje cell development. (A, B) Expression at 2.9 dpf (70 hpf) of VGlut1 (A1, B1) and Pvalb7 (A2, B2), in both dorsal and sagittal views. Merge (A3, B3) shows that VGlut1 and Pvalb7 show little overlap at this early time point. Additionally, VGlut1 expression can be found in parallel fibers that project posteriorly (A1, B1; white arrowheads). (C, D) Expression at 3.3 dpf (80 hpf) of VGlut1 (C1, D1), Pvalb7 (C2, D2) and merge (C3, D3) shows that parallel fibers expand forward, beginning to overlap with Purkinje cells during this time period. There is substantial outgrowth of parallel fibers projecting posteriorly (C1, D1; white arrowheads). (E, F) Expression at 5dpf shows that by this time point VGlut1 (E1, F1) and Pvalb7 (E2, F2) are highly spatially coordinated (merge; E3, F3) and both layers have begun to curve anteriorly. Scale bar 50 μm. Images taken using 20× (1.0 NA) water objective. [Color figure can be viewed in the online issue, which is available at wileyonlinelibrary.com.]

apparent layering of Pvalb7 and VGlut1 signal also indicative of formation of nascent circuits at these time points?

To further examine putative circuits between Purkinje cells and presynaptic parallel fibers, higher magnification images were taken to visualize morphology of individual Purkinje cells and their spatial relationship to the parallel fibers. These images were taken from a sagittal view at the most lateral portion of the cerebellum. At 3.3 dpf, VGlut1 was seen in a small layer just dorsal to the Purkinje cell bodies [Fig. 5(A2); white dashed region]. Interestingly, the layer of VGlut1 expression overlapped with the presumptive neurites expressing Pvalb7 at this time point [Fig. 5(A_1); white dashed region], strengthening the case for considering this Pvalb7 expression to represent putative developing neurites. VGlut1 expression at 5 dpf and 7dpf also highly overlapped with the developing dendritic arbor at these time points [Fig. 5(B,C)], indicating that the circuit is spatially, though not necessarily functionally, developed.

DISCUSSION

Here we have created a detailed spatiotemporal map of Purkinje cell development in the larval zebrafish cerebellum and have carefully quantified the development of the Purkinje cell layer and of individual Purkinje cells. In mapping Purkinje cell development over time, we were first able to show that Purkinje cells expressed the Pvalb7 protein, and therefore, were differentiated, as early as 2.8 dpf (67 hpf). This result allows us to narrow the precise time point of initial Purkinje cell differentiation in zebrafish to within a 12-h window between 2.3 (54 hpf) and 2.8 dpf (67 hpf). While previous studies showed that differentiation occurs by 3 dpf, our data suggest that the Purkinje cell layer is already largely present by this time point.

Our findings also show that Purkinje cell differentiation appears to be spatially regulated, beginning at 2.8 dpf with two clusters in each cerebellar hemisphere—a dorsomedial and a ventrolateral cluster. These clusters merged over the next 24–48 h, forming a continuous layer by 4 dpf. Previous studies have shown spatial and functional mediolateral compartmentalization in other cell types within the zebrafish cerebellum. Immature granule cells in the upper rhombic lip are spatially patterned into dorsomedial and ventrolateral clusters in zebrafish (Volkmann et al., 2008) that are remarkably similar to the Purkinje cell clusters observed in our investigation. These populations of granule cells were determined to represent functionally distinct compartments. To our knowledge, ours is the first report that suggests that certain populations of immature Purkinje cells are spatially compartmentalized; however, a recent study reports that the functional output of Purkinje cells in zebrafish larvae varies depending on mediolateral position within the cerebellum (Matsui et al., 2014). If such functionally distinct Purkinje cells derive from spatially distinct clusters, then these diverse populations of Purkinje cells may be distinguishable as early as differentiation, which would allow us to follow and possibly manipulate the spatial and functional development of the cerebellum.

Next, we quantified the morphological changes in the Purkinje cell layer over time by measuring various dimensions from 2.8 to 14 dpf. Quantitative analysis revealed that the majority of the gross morphological changes to the Purkinje cell layer occurred within the first 4 days of development. Purkinje cell layer anterior–posterior length increased steadily with age between differentiation and 14 dpf as more cells arrived and as the cerebellum curved anteriorally. Both Purkinje cell layer volume and cell body number, in contrast, increased logarithmically with age, with the most drastic increases in each occurring between 3 and 4 dpf, followed by smaller increases over time. This suggests that an initial, brief period of intense differentiation is followed by an immediate slowing down in the birth and/or differentiation of Purkinje cells. Such a sudden increase in Purkinje cell number between 3 and 4 dpf may be necessary to prepare the cerebellum for coordinating swimming motions in the larval fish, which begins after the fish has hatched and its swim bladder has inflated at 3 dpf (Kimmel et al., 1995). Morphological and functional changes within the cerebellum, as well as more refined motor behaviors of the fish that occur after 4 dpf, are thus more likely due to changes in the developing circuitry, and not due to the appearance of new Purkinje cell populations. It is important to note, however, that although we found evidence for a slowing down of Purkinje cell differentiation after 4 dpf, others have reported larger increases in the number of Pvalb7-expressing Purkinje cell bodies between 7 and 14 dpf (Kaslin et al., 2013). The quantitative methods varied between these two studies (sections vs. whole mounts used here). Further studies need to be done, ideally using a variety of different labeling techniques.

In our quantification of morphological changes of individual Purkinje cells, we measured a significant decrease in cell body diameter between 3.3 and 14 dpf. There are several potential explanations for this observation. Since differentiated Purkinje cells are

postmitotic, they are not reducing their cell diameter by dividing; instead, the Purkinje cell bodies could be shifting from an oblong to a more spherical morphology, decreasing the longest axis of the cell body as the cell distributes volume more evenly. Measures of cell roundness, however, demonstrated that this is not the case; in fact, cell shape became slightly more oval and elongated over time. Alternatively, cytoplasm from the cell body may be redistributed into the axons and dendrites as these processes develop. In particular, the extensive nature of growing Purkinje cell dendrites may require cytoplasmic reserves from the soma. This explanation is consistent with our data, as the decrease in cell body diameter between 3.3 and 14 dpf corresponded with a substantial increase in visible Purkinje cell dendritic tree signal. Additionally, this hypothesis would support the logarithmic nature of Purkinje cell layer volume increase that we observed; as cell diameter decreased, total cell volume was not lost, but rather redistributed while the overall region expanded. To our knowledge, there have been no other studies about the change in Purkinje cell size during zebrafish development; however, other studies on the timing of Purkinje cell dendrite outgrowth in zebrafish (Tanabe et al., 2010) are consistent with our data, supporting dendritic formation as an underlying cause of cell size decrease. In rat cerebellum, a decrease in Purkinje cell diameter was not observed during early cerebellar development, although cell body growth slowed during an intense period of dendritic spine formation (Takács and Hámori, 1994).

We were next able to quantify cell body packing in the Purkinje cell layer to determine whether cells were packing more closely together or spreading farther apart during development. By examining the average distance to each Purkinje cell's nearest neighboring cell, we found that neighbor distance increased with age between 3 and 14 dpf, indicating that cells were spreading apart slightly as the cerebellum developed. This result is consistent with work in rat cerebellum, which shows that the density of Purkinje cells in the molecular layer decreases during a roughly corresponding period of development (Takács and Hámori, 1994). During this time, Purkinje cell bodies may begin a spatial reorganization that causes them to spread apart, a process that continues in zebrafish until at least 14 dpf. Perhaps the Purkinje cells begin to assemble from a thick, unorganized multilayer of cell bodies over a relatively small area into a thin monolayer of cell bodies, as is present in the adult zebrafish cerebellum (Bae et al., 2009).

We also successfully labeled granule cell terminals, the presynaptic partner of the Purkinje cell, with the vesicular glutamate transporter type 1 (VGlut1) antibody, enabling us to view the parallel fibers that inhabit the molecular layer of the cerebellum during the first 2 weeks of development. Notably, we first detected VGlut1 expression by 2.8 dpf, which is slightly earlier than previous reports stating that granule cell markers did not appear until 3 dpf (Bae et al., 2009; Kani et al., 2010). Moreover, VGlut1 expresses in granule cell axons, and may not appear immediately following granule cell differentiation, thus our data suggest that granule cell progenitors may begin to differentiate even earlier than 2.8 dpf. Our data show that the expression of VGlut1 at the parallel fibers directly coincided with the differentiation of Purkinje cells and expression of Pvalb7. Though it is possible that VGlut1 begins to express anytime between 2.3 and 2.8 dpf, it does appear that Purkinje cell differentiation and emergence of parallel fibers are highly temporally coincident. In contrast, work in the mammalian cerebellum demonstrates that granule cells differentiate later than Purkinje cells. Immature Purkinje cells are present as early as the second embryonic week (Miale and Sidman, 1961; Altman and Bayer, 1978; Hashimoto and Mikoshiba, 2003), while differentiated granule cells in the inner granule layer are not visible until the first postnatal week and continue differentiation through the third postnatal week (Miale and Sidman, 1961; Altman and Bayer, 1997).

In addition, we saw that there appear to be two phases to parallel fiber outgrowth in the cerebellum: first, one population of granule cells extended their parallel fibers at the most posterior region of the cerebellum and out of the cerebellum into the CC, presumably to synapse with Pvalb7-expressing cell bodies, likely crest cells in the medial octavolateral nucleus. This population of granule cells appeared before 2.9 dpf, and likely represents granule cells within the EG. We show that a second population of granule cells extended their parallel fibers into the dorsomedial region of the cerebellum. This population appeared later in development, and likely corresponds to granule cells within the CCe. While our data do not allow us to conclude that there are indeed two separate granule cell populations, our findings are highly consistent with previous data that show the existence of functionally compartmentalized granule cells in the zebrafish cerebellum (Volkmann et al., 2010). Labeling granule cell bodies in addition to parallel fiber axons would help to determine whether the appearance of these two populations of parallel fibers is mirrored by the appearance of cell bodies in dorsomedial and ventrolateral clusters in the cerebellum.

To investigate possible connectivity between parallel fibers and Purkinje cells, we examined expression of VGlut1 and Pvalb7 in the developing molecular layer. First, we found that primitive Purkinje cell neurites appeared to form by 3.3 dpf, and that dendrites were present but immature in morphology by 5 dpf, then more defined by 7 dpf, with a primary dendrite and extensive branching. This timing is consistent with an existing study on zebrafish Purkinje cell morphology *in vivo* (Tanabe et al., 2010). We found that VGlut1 expression in parallel fibers and Pvalb7 expression in Purkinje cells were highly coincident beginning as early as 3.3 dpf. By this time point, parallel fibers were found dorsal to the Purkinje cells in all areas and appeared to overlap with primitive neurites potentially forming onto Purkinje cells. This suggests that the parallel fibers are in place in the molecular layer by 3.3 dpf, 2 days earlier than the Purkinje cell-granule cell synapse presumptively begins to function (Bae et al., 2009). The next 2 days may be required to establish the Purkinje cell's dendritic arbor or fine tune expression of presynaptic and/or postsynaptic components. This could be tested by labeling the metabotropic glutamate receptor subtype 1, a subtype of glutamate receptors that localizes to Purkinje cell dendrites (Gorcs et al., 1993; Janmaat et al., 2009). Alternatively, the pre- and postsynaptic components may be present but not yet precisely apposed to one another.

By 5 and 7 days, the VGlut1 expression in the parallel fibers appeared to be spatially coordinated with the localization of the Purkinje cell dendrites, raising the possibility that either the Purkinje cell dendrites grow in response to parallel fiber signals, or newly formed parallel fibers respond to Purkinje cell signals and innervate the dendritic tree as it expands. In the mammalian cerebellum, granule cells release signals that are crucial for Purkinje cell-parallel fiber synapse formation and this stimulates Purkinje dendritic growth (Cohen-Cory et al., 1991; Ito-Ishida et al., 2014). It is important to note that our characterization of the dendritic arbor and the conclusions we can draw are limited by the cellular mobility of the Pvalb7 protein. While in developed cells, Pvalb7 is found in the cytoplasm throughout the cell, it is possible that at early time points, particularly 3.3 dpf, the Pvalb7 protein had not yet dispersed into these fine processes and thus the dendrites were not yet visible. Complementary approaches for labeling newborn Purkinje cells, as well as functional studies that can identify unambiguously synaptic connections with granule cells, will be important next steps.

Our findings build upon previous work in the developing cerebellum by establishing a quantitative spatiotemporal map of Purkinje cell development in zebrafish that can be used as a metric for future studies. The maturation of the cerebellum during the first 2 weeks of zebrafish development corresponds with the appearance of coordinated behavior and movements within larvae. Development of the Purkinje cell layer likely prepares the cerebellum to help generate and refine new complex behaviors in young fish that are required for its survival during this period, such as coordinating swimming and motor reflex behaviors (Wolman and Granato, 2012). Functional behaviors such as these can be studied within the context of this detailed cerebellar timeline to help understand the underlying neural circuits that are crucial for motor control and coordination. Moreover, mutations or drugs that affect cerebellar pathways can be screened in zebrafish, using this metric as a comparison in order to quantify subtle effects.

We wish to thank L. Weston for assistance with experiments and analysis, and N. Velazquez-Ulloa, Y.P. Chen, M.C. Manzini, Y.A. Pan, and K. Cerveny for helpful discussions and comments on the manuscript. We thank K. Cerveny and Y.A. Pan for sharing fish lines and reagents, and M. Hibi for graciously providing the VGlut1 and Pvalb7 primary antibodies. The authors declare no conflicts of interest. Author Contributions: K.H. and T.W. planned experiments. K.H. carried out experiments with assistance from Z.T., and performed data analysis. K.H. and T.W. wrote the manuscript.

REFERENCES

Altman J, Bayer SA. 1978. Prenatal development in the cerebellar system in the rat I. Cytogenesis and histogenesis of the deep nuclei and the cortex of the cerebellum. J Comp Neurol 179:23–48.

Altman J, Bayer SA. 1997. Development of the Cerebellar System in Relation to its Evolution, Structure and Function. Boca Raton, FL: CRC, p 783.

Bae YK, Kani S, Shimizu T, Tanabe K, Nojima H, Kimura Y, Higashijima S, et al. 2009. Anatomy of zebrafish cerebellum and screen for mutations affecting its development. Dev Biol 330:406–426.

Bell CC. 2002. Evolution of cerebellum-like structures. Brain Behav Evol 59:312–326.

Chaplin N, Tendeng C, Wingate RJ. 2010. Absence of an external germinal layer in zebrafish and shark reveals a distinct, anamnioate ground plan of cerebellum development. J Neurosci 30:3048–3057.

Cohen-Cory S, Dreyfus CF, Black IB. 1991. NGF and excitatory neurotransmitters regulate survival and morphogenesis of cultured cerebellar Purkinje cells. J Neurosci 11:462–471.

Corrales JD, Blaess S, Mahoney EM, Joyner AL. 2006. The level of sonic hedgehog signaling regulates the complexity of cerebellar foliation. Development 133:1811–1821.

Corrales JD, Rocco GL, Blaess S, Guo Q, Joyner AL. 2004. Spatial pattern of sonic hedgehog signaling through Gli genes during cerebellum development. Development 131: 5581–5590.

Fatemi SH, Aldinger KA, Ashwood P, Bauman ML, Blaha CD, Blatt GJ, Chauhan A, et al. 2012. Consensus paper: Pathological role of cerebellum in autism. Cerebellum 11:777–807.

Fleming JT, He W, Hao C, Ketova T, Pan FC, Wright CCV, Litingtung Y, et al. 2013. The Purkinje neuron acts as a central regulator of spatially and functionally distinct cerebellar precursors. Dev Cell 27:278–292.

Goldowitz D, Hamre K. 1998. The cells and molecules that make a cerebellum. Cerebellum 21:375–382.

Gorcs TJ, Penke B, Katarova Z, Hámori J. 1993. Immunohistochemical visualization of a metabotropic glutamate receptor. Neuroreport 4:283–286.

Gosalakkal JA. 2001. Ataxias of childhood. Neurologist 7: 300–306.

Hall ZJ, Street SE, Healy SD. 2013. The evolution of cerebellum structure correlates with nest complexity. Biol Lett 9:20130687.

Hashimoto M, Mikoshiba K. 2003. Mediolateral compartmentalization of the cerebellum is determined on the "birth date" of Purkinje cells. J Neurosci 23:11342–11351.

Hibi M, Shimizu T. 2012. Development of the cerebellum and cerebellar neural circuits. Dev Neurobiol 72:282–301.

Hoshino M. 2006. Molecular machinery governing GABAergic neuron specification in the cerebellum. Cerebellum 5:193–198.

Hoshino M, Nakamura S, Mori K, Kawauchi T, Terao M, Nishimura YV, Fukuda A, et al. 2005. Ptf1a, a bHLH transcriptional gene, defines GABAergic neuronal fates in cerebellum. Neuron 47:201–213.

Ito-Ishida A, Okabe S, Yuzaki M. 2014. The role of cbln1 on Purkinje cell synapse formation. Neurosci Res 83:64–68.

Iwaniuk AN, Lefebvre L, Wylie DR. 2009. The comparative approach and brain-behavior relationships: A tool for understanding tool-use. Can J Exp Psychol 63:150–159.

Janmaat S, Frederic F, Sjollema K, Luiten P, Mariani J, van der Want J. 2009. Formation and maturation of parallel fiber-purkinje cell synapses in the staggerer cerebellum ex vivo. J Comp Neurol 512:467–477.

Kani S, Bae YK, Shimizu T, Tanabe K, Satou C, Parsons MJ, Scott E, et al. 2010. Proneural gene-linked neurogenesis in zebrafish cerebellum. Dev Biol 343:1–17.

Kaslin J, Kroehne V, Benato F, Argenton F, Brand M. 2013. Development and specification of cerebellar stem and progenitor cells in zebrafish: From embryo to adult. Neural Dev 8:1–15.

Kimmel CB, Ballard WW, Kimmel SR, Ullmann B, Schilling TF. 1995. Stages of embryonic development of the zebrafish. Developmental Dynamics 203:253–310.

Köster RW, Fraser SE. 2006. FGF signaling mediates regeneration of the differentiating cerebellum through repatterning of the anterior hindbrain and reinitiation of neuronal migration. J Neurosci 26:7293–7304.

Lewis PM, Gritli-Linde A, Smeyne R, Kottmann A, McMahon AP. 2004. Sonic hedgehog signaling is required for expansion of granule neuron precursors and patterning of the mouse cerebellum. Dev Biol 270:393–410.

Lieschke GJ, Currie PD. 2007. Animal models of human disease: Zebrafish swim into view. Nat Rev Genet 8:353–367.

Lisney TJ, Yopak KE, Montgomery JC, Collin SP. 2008. Variation in brain organization and cerebellar foliation in chondrichthyans: Batoids. Brain Behav Evol 72:262–282.

Matsui H, Namikawa K, Babaryka A, Köster RW. 2014. Functional regionalization of the teleost cerebellum analyzed in vivo. Proc Natl Acad Sci USA 111:11846–11851.

Merzin M. 2008. Applying stereological method in radiology. Volume measurement. Bachelor's thesis. University of Tartu.

Miale IL, Sidman RL. 1961. An autoradiographic analysis of histogenesis in the mouse cerebellum. Exp Neurol 4: 277–296.

Miyamura Y, Nakayasu H. 2001. Zonal distribution of Purkinje cells in the zebrafish cerebellum: Analysis by means of a specific monoclonal antibody. Cell Tissue Res 205: 299–305.

Nüsslein-Volhard C, Dahm R. 2002. Zebrafish. Oxford University Press Inc., New York.

Picard H, Amado I, Mouchet-Mages S, Olié J-P, Krebs M-O. 2008. The role of the cerebellum in schizophrenia: An update of clinical, cognitive, and functional evidences. Schizophr Bull 34:155–172.

Takács J, Hámori J. 1994. Developmental dynamics of Purkinje cells and dendritic spines in rat cerebellar cortex. J Neurosci Res 38:515–530.

Tanabe K, Kani S, Shimizu T, Bae YK, Abe T, Hibi M. 2010. Atypical protein kinase c regulates primary dendrite specification of cerebellar purkinje cells by localizing golgi apparatus. J Neurosci 30:16983–16992.

van Welie I, Smith IT, Watt AJ. 2011. The metamorphosis of the developing cerebellar microcircuit. Curr Opin Neurobiol 21:245–253.

Volkmann K, Chen Y-Y, Harris MP, Wullimann MF, Köster RW. 2010. The zebrafish cerebellar upper rhombic lip generates tegmental hindbrain nuclei by long-distance migration in an evolutionary conserved manner. J Comp Neurol 518:2794–2817.

Volkmann K, Rieger S, Babaryka A, Köster RW. 2008. The zebrafish cerebellar rhombic lip is spatially patterned in producing granule cell populations of different functional compartments. Dev Biol 313:167–180.

Wechsley-Reya RJ, Scott MP. 1999. Control of neuronal precursor proliferation in the cerebellum by sonic hedgehog. Neuron 22:103–114.

Westerfield M. 2000. The Zebrafish Book: A Guide for the Laboratory Use of Zebrafish (*Danio rerio*), 4th ed. Eugene, OR: The University of Oregon Press.

White JJ, Arancillo M, Stay TL, George-Jones NA, Levy SL, Heck DH, Sillitoe RV. 2014. Cerebellar zonal patterning relies on Purkinje cell neurotransmission. J Neurosci 34:8231–8245.

Wolman M, Granato M. 2012. Behavioral genetics in larval zebrafish: Learning from the young. Dev Neurobiol 72: 366–372.

Yanicostas C, Barbieri E, Hibi M, Brice A, Stevanin G, Soussi-Yanicostas N. 2012. Requirement for zebrafish ataxin-7 in differentiation of photoreceptors and cerebellar neurons. PloS One 7:1–13.

Yuasa S, Kawamura K, Ono K, Yamakuni T, Takahashi Y. 1991. Development and migration of Purkinje cells in the mouse cerebellar primordium. Anat Embryol 184:195–212.